Thermal desorption technique to speciate mercury in carbonate, silicate, and organic-rich soils

Federica Meloni [a,b,*], Pablo L. Higueras [c], Jacopo Cabassi [b], Barbara Nisi [b], Daniele Rappuoli [d,e], Orlando Vaselli [a,b]

[a] Department of Earth Sciences, Via G. La Pira, 4 – 50121, Firenze, Italy
[b] CNR-IGG Institute of Geosciences and Earth Resources, Via G. La Pira, 4 – 50121, Firenze, Italy
[c] Instituto de Geología Aplicada, Universidad de Castilla-La Mancha, Pl. Manuel Meca 1, 13400, Almadén, Ciudad Real, Spain
[d] Unione dei Comuni Amiata Val d'Orcia, Unità di Bonifica, Via Grossetana 209, 53025, Piancastagnaio, Siena, Italy
[e] Parco Museo Minerario di Abbadia San Salvatore - Via Suor Gemma, 53021, Abbadia San Salvatore 1, Siena, Italy

HIGHLIGHTS

- Mercury speciation in different soil matrices by Lumex-Pyro 915+.
- Desorption temperatures of Hg compounds are dependent on the Hg-bearing matrix.
- Hg^0 suffers oxidation processes to form more stable species Hg^{2+} in $t_{1/2}$–42 days.
- Results may have important implications during soil remediation activities.

GRAPHICAL ABSTRACT
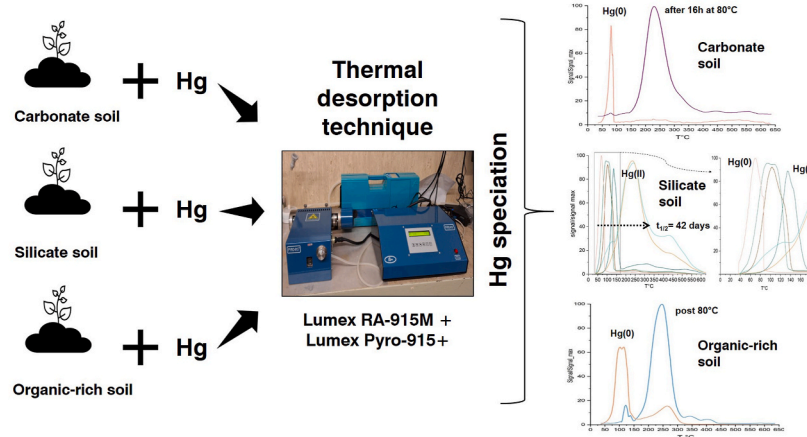
ARTICLE INFO

ABSTRACT

Thermal desorption is a well-assessed technique to speciate mercury (Hg) in soils and sediments. However, the effects related to the different matrices are still not properly assessed. In this study, thermal desorption was applied to Hg-free calcite mixed with Hg standard and soils rich in carbonate and silicate minerals, as well as organic matter. Hg^0, $HgCl_2$, HgO, α-HgS, β-HgS and organo-mercuric compounds were recognized, pointing out that the soil matrix operates notable differences in terms of breakdown temperatures of the Hg-compounds and suggesting that the mineralogical composition of soil has to be investigated before applying the thermal desorption technique. Furthermore, the presence of ^{Hg0} was carefully evaluated since, as already observed, it forms Hg^{2+}, which increases mercury mobility in the pedological cover with important consequences for those

---

* Corresponding author. Department of Earth Sciences, Via G. La Pira, 4 – 50121 Firenze, Italy.
E-mail addresses: federica.meloni@unifi.it (F. Meloni), pablo.Higueras@uclm.es (P.L. Higueras), jacopo.cabassi@igg.cnr.it (J. Cabassi), barbara.nisi@igg.cnr.it (B. Nisi), d.rappuoli@uc-amiatavaldorcia.si.it (D. Rappuoli), Orlando.vaselli@unifi.it (O. Vaselli).

soils contaminated and located close to decommissioned or active mining areas and/or industrial sites (e.g. chloro-alkali industries). Experimental runs were thus carried out by using carbonate-, silicate- and organic-rich soils doped with liquid Hg. It was observed that Hg^0 tends to be oxidized to form Hg^+ and then Hg^{2+} as a function of soil matrix and reaction time. Surprisingly, the oxidation rate is rather fast, since after 42 days the initial content of Hg^0 is halved, thus following an exponential decay. This implies that in Hg^0-polluted areas, the fate of the resulting Hg^{2+} can be that to: i) be adsorbed by organic matter and/or Fe–Mn–Al oxides and/or ii) feed shallow aquifers. This study is a further step ahead to understand the behavior of Hg in contaminated soils from industrial and mining areas where liquid Hg is occurring in different soil matrices and may provide useful indications for remediation operations.

1. Introduction

Mercury (Hg) is ranked among the ten chemicals of concern by WHO (2017). It has been estimated that approximately 86 Gg of anthropogenically-derived Hg are distributed in surface soils at global scale (UNEP, 2009). There is a tight relationship between the chemical form of Hg and its toxicity (in particular methylmercury, e.g. Hong et al., 2012; Dong et al., 2016; Wu et al., 2024) to humans (Liu et al., 2020). Mercury in soils may occur as Hg^0, Hg_2^{2+}, Hg^+, and Hg^{2+} and its speciation is affected by several factors such as reactivity (pH), redox potential (Eh) and soil organic matter (hereafter SOM) contents. Clays, iron, sulfur, phosphorus, and carbon are also able to influence the distribution of Hg in solid matrices, whose speciation can thus be relatively variable (Widmöller et al., 2017). The main sources of Hg in soil are due to both natural and anthropogenic emissions. Natural sources are related to rock weathering (Liu et al., 2020) and volcanic and geothermal emissions, whereas Hg emissions from industrial activities (e.g. chloro-alkali), coal combustion, as well as precious metal extraction in industrial and small-scale gold mining (e.g. AMAP/UNEP, 2013; Mason et al., 2012, Driscoll et al., 2013), are the main anthropogenic sources.

The main Hg-bearing ore sources in soil are cinnabar and meta-cinnabar which are practically insoluble in water (Ariya et al., 2015). Their solubility product (K_{ps}) is indeed equal to $2*10^{-53}$ and $2*10^{-52}$ mol/L, respectively (Chen et al., 2018), meaning that they are not prone to be chemically altered at exogenous conditions, differently by other Hg species, such as $HgCl_2$ (K_{ps}: 0.27 mol/L; Ariya et al., 2015). Consequently, the pivotal assessment of potential impact on humans and ecosystems has to be focused on defining how Hg is speciated in different environmental matrices.

One of the main challenges to face during remediation operations in Hg-contaminated soils is to assess whether gaseous elemental Hg and/or liquid Hg occur. While atmospheric Hg^0 (Gaseous Elemental Mercury, hereafter GEM) is considered a global pollutant, due to its scarce solubility in water and its relatively long residence time (from 0.8 to 1.7 years, Ariya et al., 2015), atmospheric Hg^{2+} (Reactive Gaseous Mercury, hereafter RGM) is promptly removed and settled on the surface through wet and/or dry deposition (Lin et al., 2010). When GEM is oxidized to RGM and deposited on the soil, it becomes part of the soil matrix, and inorganic mercuric salts and minerals such as $HgCl_2$, HgO, or HgS and/or organo-mercuric compounds can be formed (O'Connor et al., 2019). On the other hand, GEM turns out to be the main route of Hg accumulation in plants (e.g. Molina et al., 2006; Meloni et al., 2023), forest soils and aquatic systems, as dissolved gaseous mercury (Wang et al., 2015), being volatile and susceptible to oxidation. Therefore, the effectiveness and success of remediation procedures are heavily depending on the mercury species that are present in the soil and the physicochemical features affecting Hg mobility are critical (Rumayor et al., 2017). In particular, when Hg occurs in a relatively mobile chemical state, soil washing is one of the preferred options to remove the contaminant (Wang et al., 2020). Differently, when mercury is firmly bonded to the soil matrix and thus, more stable, it is released more slowly (Xu et al., 2015).

Over time, various analytical approaches (e.g. sequential or selective extractions, thermal desorption: TD) have been devised for the detection of different Hg species in solid matrices (e.g. Widmöller et al., 2017; Petranich et al., 2022; Ghezzi et al., 2023). Nevertheless, TD (Biester, 1994) seems to be the most appropriate, less time-consuming, and less costly technique for powdered samples to determine and qualitatively detect the speciated Hg phases, particularly when they are at low concentrations (Sladek and Gustin, 2003; Rumayor et al., 2017; Widmöller et al., 2017). Kinetic processes and vaporization mechanisms are partly reflected in the different behavior of the Hg species during TD. However, there is no direct relationship between desorption temperatures and physicochemical characteristics of pure Hg compounds, such as melting, sublimation point, and vapor pressure (Widmöller et al., 1996). During the TD process, heating (from 50 to 800 °C) breaks the Hg bonds (in both rocks or soil) and then, the metal in its elemental gaseous state is released as a function of the bond strength (Biester, 1994).

While the quantification of the various Hg species can be determined by TD, the amount of elemental Hg present in the solid matrix can be computed by comparing the Hg concentration between heated and not heated samples (Sladek and Gustin, 2003; Bouffard and Amyout, 2008; Padalkar et al., 2019; Friani et al., 2023). At temperatures between 50 and 100 °C, the Hg species with low oxidation states (Hg^0 and Hg^+) are generally released. Different heating temperatures and times (i.e. 80 °C for 8 h and 150 °C for 2 h) are commonly used to remove Hg^0. However, when the Hg^0 fraction is low, this analytical approach has poor reproducibility and precision (Ghezzi et al., 2023). A crucial point in remediation actions of Hg-contaminated sites is to identify the presence and the amount of Hg^0 in soils as precisely as possible. Even though Hg has low solubility (e.g. Ariya et al., 2015), when oxidation processes occur, soluble species (e.g. Hg^{2+}) may form and the Hg mobility in the environment is favored (Widmöller et al., 2015). As a result, interventions on soils from contaminated areas (such as Hg-mining areas, chlor-alkali plants, and PVC industries) are strictly depending on the available different species of Hg (Raposo et al., 2023). Soils are a potential reservoir of PTEs (Potentially Toxic Elements; e.g. Ghani et al., 2024), including Hg (Obrist, 2012). Chemical processes and those induced by bacterial community favor the transformation of the available Hg-inorganically bound into organic forms (e.g. Obrist et al., 2018; Huang et al., 2023). In Hg-contaminated soils, these processes may affect the vegetation (e.g. Azevedo and Rodriguez, 2012).

To the best of our knowledge, TD experimental runs aimed at investigating Hg speciation in uncontaminated silicate, carbonate, and peat soil samples doped with known contents of both liquid Hg (Hg_l^0) and Hg-standards ($HgCl_2$, $HgSO_4$, β-HgS – metacinnabar – and α-HgS – cinnabar) at different times and temperatures have not systematically been carried out. Liquid Hg in soils, as uncoated or coated Hg_l^0 beads, can be found close to decommissioned cinnabar roasting areas or industrial complexes (e.g. chloro-alkali) or where liquid Hg spills occurred (e.g. Miller et al., 2015; Du et al., 2023). Therefore, after defining the breaking-temperature for each Hg-standards, the main goals of our study can be summarized, as follows: i) assess whether the different matrices are able to affect the release of Hg^0; ii) verify whether the addition of Hg_l^0 is favoring the formation of new Hg species at environment temperatures, and iii) study the dynamics of Hg species after the incorporation of Hg_l^0 into the soil. All the experiments were conducted by TD.

2. Materials and methods

2.1. Equipment

The content of total Hg (THg) and Hg speciation were determined with a Lumex RA-915 M (Atomic Absorption Spectrometry with Zeeman effect) instrument coupled with a Lumex Pyro-915+ device by using a heating step procedure (Sholupov et al., 2004; Mashyanov et al., 2017). The Pyro-915+ device consists of a furnace with two connected chambers. In the first chamber, the temperature is continuously monitored by a thermocouple placed inside a quartz boat. Here, solid, or liquid samples are pyrolyzed or volatilized, respectively. In the second chamber, the temperature is kept at about 800 °C to reduce all the Hg compounds to elemental Hg and eliminate the interferent species, while the resulting fumes are abated by an activated charcoal cartridge (Rumayor et al., 2013). In the present study, in the first chamber, a heating ramp with three different steps was selected to warm-up the instrument (temperature from 36 °C to 635 °C). In the first step, the temperature was kept at 28.8 °C min^{-1} for 140 s and then, increased from 36 °C to 148.8 °C). In the second step, the temperature was regulated at 40.8 °C min^{-1} for 340 s and successively, increased up to 480 °C. The temperature was then held at 49.8 °C min^{-1} for 360 s in the third step and eventually, the final temperature was set at 635 °C.

Hg-free air was used as carrier gas with a flow rate of ca. 3 L min^{-1}. The certified material NIST 2711a (Montana Soil II) (Hg mass fraction = 7.42 ± 0.18 mg/kg) was measured (the recovery was equal to 98.11–102.3%) to guarantee quality control and calibrate the device. In addition, the NIST 2711a was analyzed three times using the TD technique (RSD <5%), to verify the precision of the heating ramp used for speciation.

2.2. Standard Hg compounds and Hg-free samples

To determine and confirm the results of previous studies on the desorption temperature and profile of the Hg compounds, Hg minerals, and synthetic compounds such as $HgCl_2$ and $HgSO_4$ (PanReac AppliChem), synthetic β-HgS, and α-HgS from the Almadén mine (Spain) with a total Hg (THg) concentration up to 800 mg/kg and some droplets of distilled liquid Hg (ca. 100 mg/kg) from the former Abbadia San Salvatore (volcanic complex of Mt. Amiata, central Italy; e.g. Vezzoli and Principe, 2023) mine were mixed and gently grinded and homogenized for 30 min under safe laboratory conditions with an agate planetary ball mill with Hg-free powdered pure calcite and a silicate soil (THg = 0.0065 mg/kg) which was collected from the Municipality of Ciudad Real (Spain). A few droplets of liquid Hg, were also mixed and homogenized with powdered carbonate (THg = 0.0006 mg/kg) and the previously mentioned silicate soils to investigate its behavior with different chemical compositions which were determined by XRF (X-Ray Fluorescence). In the carbonate soil, the percentage of $CaCO_3$ was calculated by using the Dietrich-Früling calcimeter. The results of XRF and calcimetry are reported in the Supplementary Material 1.

2.3. Determination of Hg^0 in soil samples by gravimetry

The Hg^0 concentration in soils and sediments can be determined by comparing heated and non-heated samples. Previous studies by Protano and Nannoni (2018) and Friani et al. (2023) quantified the concentration of Hg^0 by determining the concentration of THg, after heating the sample at 30 °C by subtracting that measured after heating at 80 °C for 16 h. Therefore, a silicate soil (S150), developed on the volcanic products of Mt. Amiata and characterized by a relatively high concentration of THg (13 mg/kg), was analyzed according to Protano and Nannoni (2018) and Friani et al. (2023). The same soil was also analyzed with TD to verify at which temperature the release of gaseous Hg after heating at 30 °C and at 80 °C (for 16 h) occurred. This soil was also heated at 80 °C for 4 days to verify whether Hg^0 was still present or new Hg species formed.

2.4. Experimental dynamics with liquid mercury

In order to verify the effective presence of Hg^0 and the possible reactions between Hg_l^0 and soil matrix, the former was also amalgamated with the Hg-free silicate soil. Specifically, one drop of Hg_l^0 was added to 10 g of silicate, carbonate and Hg-free peat (THg = 0.0003 mg/kg) soils. Then, as previously described, each soil type was ground and homogenized. Afterward, 30 mg of each soil was analyzed by TD at which temperature the gaseous Hg was released. Once this procedure was completed, 1 g of silicate soil was placed in an oven at 80 °C for 16 h to observe any changes in terms of chemical speciation of Hg and verify the reliability of the gravimetric method for the determination of Hg^0. Furthermore, to establish if Hg_l^0 was associated with soil organic matter (SOM), 0.5 mg of each post-heated (at 80 °C) soil was left reacting with 10 mL of suprapur H_2O_2 (Sigma Aldrich®) to destroy the organic matter. Once the effervescence ceased, indicative of SOM consumption, each solution was transferred to a 15 mL falcon-like vial and centrifuged at 5000 rpm to separate the supernatant from the solid phase. Subsequently, the solid was then recovered and dried at 30 °C. The three soil samples were again analyzed for the determination of THg and Hg speciation.

3. Results

3.1. Mercury speciation by thermal desorption: pure and natural compounds

The thermal desorption profiles (TDPs), or thermograms, were used to identify each Hg species as Hg^0 was formed during the heating process. Each TDP displays the temperature at which the thermal release of Hg^0 begins, reaches its maximum, and then drops back to the baseline. Then, the peak temperature corresponds to the maximum release of Hg^0 and it is specific for each Hg-species occurring in the analyzed sample (Rumayor et al., 2013). The thermograms related to synthetic and natural Hg standards mixed with pure calcite and silicate soil are reported in Fig. 1A and B, respectively, where the peak signal corresponds to a distinctive temperature, characterizing the different Hg-bearing phases. The corresponding temperature of each Hg compound is listed in Table 1.

As illustrated in Fig. 1A and B, the release temperature of Hg^0 from the solid mixtures between pure calcite and silicate soil with the Hg standards is ranging from 70 to 100 °C. $HgCl_2$, as relatively volatile Hg compound, tends to sublimate at low temperatures (Wu et al., 2015). The release temperature of $HgCl_2$ is indeed <180 °C. The thermograms obtained for the α-HgS from Almadén, mixed with pure calcite and silicate soil, and for synthetic β-HgS in silicate soil, are similar to those reported by Petranich et al. (2022). $HgSO_4$ is characterized by two peaks: a) the first one is a weak signal at relatively low temperatures (at 322 and 356 °C, for calcite and silicate soils, respectively) and b) the second one is at higher temperature with a well-marked signal (high-temperature peak 531 and 459 °C, for calcite and silicate soils, respectively).

4. Discussion

The thermograms of Fig. 1A and B evidence that Hg^0 is completely released between 70 and 90 °C, as also demonstrated by Biester and Scholz (1996), independently by the soil matrix. Differently, when synthetic and natural Hg compounds mixed with pure calcite and silicate soils are analyzed, the Hg-desorption temperature is significantly influenced by the mineralogical composition of soil in agreement with Petranich et al. (2022). Most Hg-species show a temperature breakdown which varies from 10 to 20 °C up to about 50 °C (e.g. $HgCl_2$) when the thermograms of Fig. 1A are compared with those of Fig. 1B.
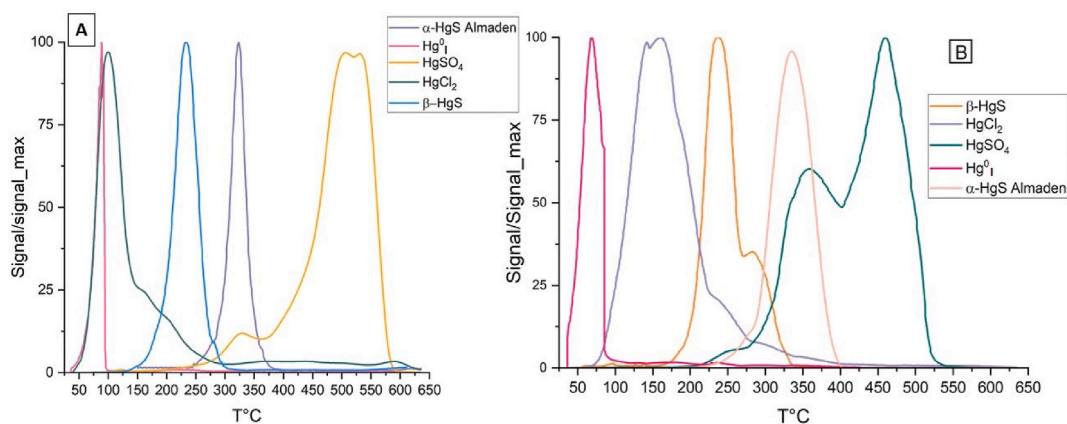
Fig. 1. A) Thermograms of synthetic and natural Hg compounds mixed with pure calcite; B) thermograms of pure Hg compounds (distilled liquid Hg, HgCl₂, HgSO₄, β-HgS and α-HgS) mixed with silicate soil.

Table 1

Thermal desorption temperatures: Hg-compounds and respective thermal dissociation temperatures mixed with pure calcite or silicate soils. The last column reports the temperature interval for each peak (start and end).

Hg-compound	High T °C peak	Thermal decomposition peak (°C)
Hg^0 mixed with pure calcite	88 ± 10	36–100
Hg^0 mixed with silicate soil	70 ± 10	36–125
$HgCl_2$ mixed with pure calcite	100 ± 5	50–275
$HgCl_2$ silicate soil	156 ± 10	80–350
Synthetic β-HgS mixed with pure calcite	233 ± 10	125–300
Synthetic β-HgS mixed with silicate soil	240 ± 8	175–350
α-HgS Almadén mixed with pure calcite	323 ± 10	250–375
α-HgS Almadén mixed with silicate soil	340 ± 11	250–400
$HgSO_4$ pure calcite	322 ± 10; 531 ± 8	250-345; 383-600
$HgSO_4$ silicate soil	356 ± 3; 459 ± 10	227-395; 400-550

Interestingly, while no significant temperature variation is found for β-HgS in the two matrices, a difference of about 20 °C is highlighted when the highest temperature peaks for α-HgS are compared. Similar results were reported by Petranich et al. (2022) since a consistent temperature range (213–236 °C) is recorded for β-HgS, while that of α-HgS is significantly affected by the soil matrix. On the contrary, HgSO₄ shows a higher desorbing temperature when the pure calcite sample is compared with those consisting of a silicate matrix (Table 1). In both matrices, two temperature peaks are highlighted during TD, as also evidenced by Rumayor et al. (2013) and Widmöller et al. (2017). According to Rumayor et al. (2013), the two thermal steps are likely related to the dissociation process of HgSO₄ due to the formation of more unstable intermediate products (i.e. HgSO₄ × 2HgO). The difference observed for the first peak between the two matrices may suggest that calcite is able to partly inhibit the formation of intermediate compounds such as HgSO₄ × 2HgO.

4.1. Experimental dynamics with liquid mercury

The gravimetric method to determine the presence of Hg^0 in soil by Protano and Nannoni (2018) and Friani et al. (2023) suggested that the soil sample S150 had a Hg^0 content of 3.2 mg/kg, which corresponded to 24.62% of THg. The same sample was analyzed by TD and then, two replicates after 16 h and 4 days at 80 °C were also performed. Basically, no Hg^0 or changes in terms of speciation can be observed in the S150

sample (Fig. 2). This indicates that the gravimetric method is likely affected by either some analytical errors or Hg^0 is tightly bound to the soil matrix (Coufalík et al., 2014) whose release temperature could be much higher. However, this experiment strengthens the good reproducibility of the TD technique.

The soil sample S150 is characterized by two peaks (at 260 °C and 329 °C, respectively), with the first one overlapping, though slightly, with the second one, corresponding to β-HgS and α-HgS, respectively. Consequently, no peak relative to the presence of Hg^0 occurs for the temperature interval between 80 and 100 °C, as instead shown in Fig. 1A and B.

The effective presence of Hg^0 and the possible reactions between Hg^0_l and the soil matrix are critical points for those areas where Hg was produced after cinnabar roasting. Liquid Hg droplets may indeed be still present and dripping from the condensers and collection pools, as in the case of the Hg-district of Mt. Amiata (Vaselli et al., 2017, 2021; Meloni et al., 2023). Consequently, investigating the interaction between liquid Hg and soil is important even for future remediation activities, since the methodological approach to remove Hg can substantially be different based on the different Hg species (Widmöller et al., 1996; Reis et al., 2016; Rumayor et al., 2017).

The results of the experimental runs are summarized in the thermogram of Fig. 3, where Hg^0, detectable in the soil after 16 h at 80 °C, is oxidized to Hg^{2+}, to form a more stable Hg phase, with two breakdown temperatures at 240 °C and 430 °C, respectively. By comparing this thermogram with those of Fig. 1B, the first peak is likely associated with
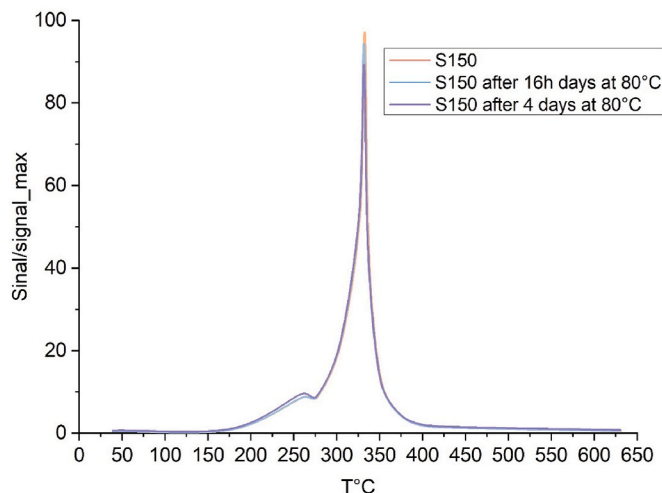

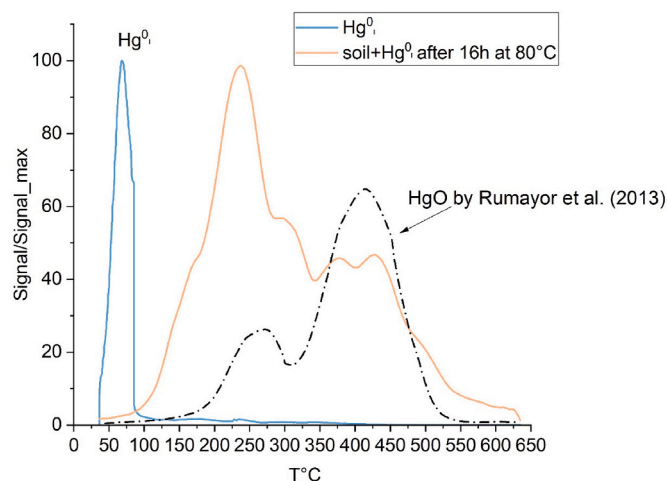
Fig. 2. Thermogram of the soil sample S150.

Fig. 3. Thermogram of Hg^0, and silicate soil mixed with Hg^0 after heating at 80 °C for 16 h.

β-HgS, while the second one pertains to either $HgSO_4$ or HgO (Rumayor et al., 2013). According to Biester et al. (1999), $HgSO_4$ is unstable under environmental conditions and the main characteristic peak at 459 ± 10 °C is not present (see Fig. 1B). Therefore, it is reasonable to assume that the second peak can be related to the thermal decomposition of newly formed HgO. The oxidative process affecting Hg^0 to form Hg^{2+} was already highlighted by many authors (e.g. Widmöller et al., 1996; Do Valle et al., 2006; Widmöller et al., 2015; Gonzalez-Raymat et al., 2017) and it depends on i) temperature conditions during sampling storage, ii) redox reactions of Hg in soils induced by light and/or UV light, iii) presence of SOM, and iv) microbial activity.

To evaluate the time necessary for Hg^0 to react with a silicate matrix and approach the TDP of Fig. 3 (orange line), the silicate soil + Hg_l^0 mixture was placed in the laboratory at about 30 °C (T = 25 ± 10 °C), representative of the Mediterranean spring to summer time, for about 6 months. The experiments started on April 25, 2023 and ended on October 10, 2023, during which 6 distinct TPDs were carried out after 1, 13, 18, 35, 65 and 167 days (Fig. 4). Hg^0 turned to be almost completely

oxidized to Hg^{2+} (Fig. 4A). According to Widmöller et al. (2015), Hg^0 is firstly oxidized to Hg^+ and subsequently to Hg^{2+}. An inset of the thermal profiles at different times is reported in Fig. 4B. Basically, in less than two weeks, the oxidation of Hg^0 begins and Hg^+ is formed. According to several studies (e.g. Rumayor et al., 2013; Petranich et al., 2022), the temperature of 114 ± 5 °C corresponds to the TD of Hg_2Cl_2, where mercury is in the form of Hg^+. After two months, some Hg^+ is still present. By calculating the first-order half-life ($t_{1/2}$) of the percentage of oxidized Hg^0 (Widmöller et al., 2015), 42 days are required, which is the time within half of the initial amount of Hg^0 has been oxidized. The complete oxidation process of Hg^+ to Hg^{2+} (99.2% of Hg^0 oxidized) (Fig. 4B) is accomplished in almost three months. In Fig. 4A, it can be seen that HgO, as evidenced in Fig. 3, tends to progressively disappear, possibly due to either the effect of UV light, according to reaction (1):

$$HgO \xrightarrow{UV} Hg^0 + O_2 \qquad (1)$$

and/or the action of sulfur-reducing bacteria and porewater (Miller et al., 2015). Mixing between Hg_l^0 and soil at ambient temperature results in the formation of HgO crystallites on the surface of the liquid mercury. However, it is important to note that the presence of HgO crystallites under these conditions does not necessarily imply that HgO will be the dominating form of mercury in areas contaminated by liquid mercury. HgO is indeed a relatively soluble salt (Ksp, $10^{-3.6}$ mol/L, Hocsman et al., 2006).

In water, Hg^{2+} ions are released from HgO and form strong complexes with various substances such as organic matter, sulfur, and oxyhydroxides of iron (Fe) and manganese (Mn), as demonstrated by Widmöller et al. (2017), Skyllberg (2008), Miller et al. (2013), and Widmöller et al. (2015). The formation of such complexes is likely playing a significant role in the mobility and bioavailability of mercury in contaminated environments. Further studies to better characterized the Hg^+-bearing phase and the presence of microbial community are required. In the latter case, Hg^{2+}-resistant bacteria are found in environments where Hg occurs. They may indeed operate to produce Hg^0 by Hg^{2+} and Hg-methylated forms (Baldi et al., 1987). Several studies (e.g. Barnett et al., 2001; Fritsche et al., 2008; Frohne et al., 2012; Cabassi et al., 2020, 2021) have indeed invoked such microorganisms to explain anomalies of Hg^0 in different environments.

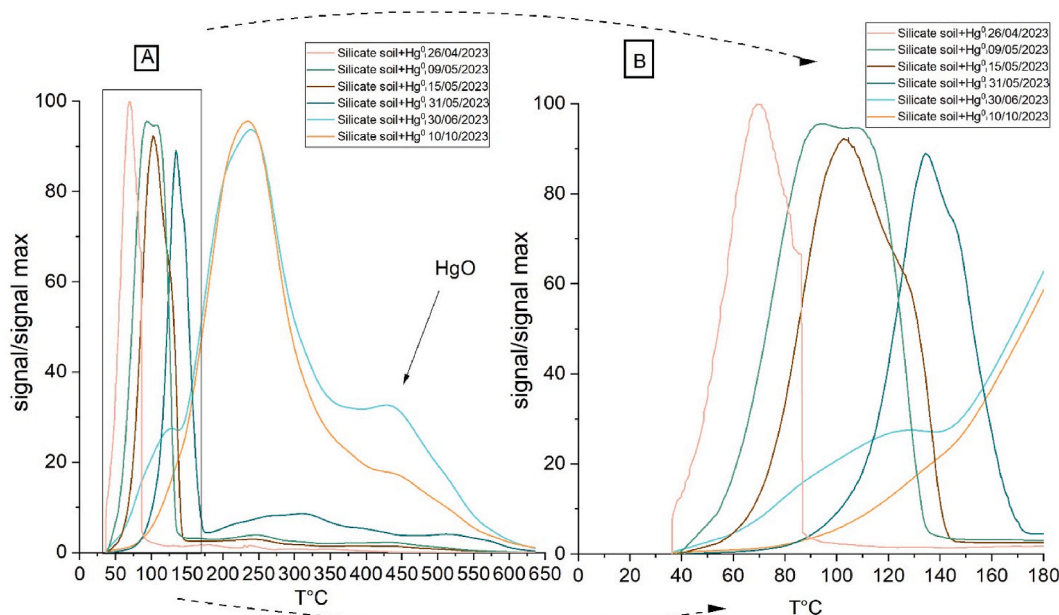This is also supported by the total Hg concentration. In June 2023,

Fig. 4. A) Thermograms of silicate soil and Hg_l^0 mixture carried out at room temperature from April to October 2023; B) inset of the previous thermogram up to 180 °C.

the THg concentration was indeed 100 mg/kg and after about three months the soil had lost almost 40 % of the THg, decreasing to 60.5 mg/kg. Gonzalez-Raymat et al. (2017), O'Connor et al., 2019, and Debure et al. (2020) stated that Hg^{2+} stabilizes in soils, being adsorbed by SOM and/or minerals (Fe, Mn, and Al oxides). In particular, the presence of SOM and Fe^{3+} promotes the oxidation of Hg^0. Groups including carboxylic acid (-COOH), phenols ($-C_6H_5OH$), hydroxides (-OH), sulfhydryl (-SH), and amines ($-NH_2$) are commonly present in soil-bearing SOM. The strong Hg^{2+}-sulfur (Hg-SR) bonds, found in naturally occurring organic matter, as well as the Hg^{2+} reaction with inorganic sulfides, was reported by Nagy et al. (2011) and Skyllberg and Drott (2010). Comparing the desorption temperatures of the first (240 °C) peak with those of β-HgS (Table 1), they appear to be similar. Therefore, we can assume that during the oxidation process, Hg_l^0 forms Hg^{2+} ions that bind with sulfur in soil to form β-HgS. It is also worth noting that the reaction between Hg_l^0 and elemental sulfur in a planetary mill after 15 min at 29 °C produces β-HgS (López et al., 2010). This further supports the hypothesis that this first peak (240 °C) is likely associated with Hg^{2+} species.

The temperature profiles after the addition of i) Hg-free $CaCO_3$ soil and ii) peat soil after the addition of Hg_l^0 are reported in Fig. 5A and B, respectively.

According to Fig. 5 A and 5B, the release temperature of Hg^0 for the Hg_l^0 + carbonate soil and Hg_l^0 + peat mixtures is between 35 and 110 °C (Fig. 5), as also evidenced for the Hg_l^0 and silicate soil mixture (Fig. 3). After 16 h at 80 °C, the main peak of Hg^0 for both mixtures disappears and a newly formed peak at 240 °C is produced (Fig. 5), probably due to the formation of β-HgS. It is to be mentioned that no peak is found at 430 °C, which was previously associated with HgO (Fig. 3). We can hypothesize that the different soil composition was able to significantly inhibit the formation of HgO. In the peat soil, a peak at 125 ± 10 °C is also present. This peak can be interpreted as related to a not-fully-oxidized Hg species, such as the unstable Hg^+. In fact, Hg^+ tends to form metal-metal bond to produce Hg_2^{2+}. According to Schuster (1991) and Gonzalez-Raymat et al. (2017), Hg_2^{2+} is quickly disproportioned into Hg^{2+} and Hg^0, and subsequently they bind to other soil components (e.g. SOM and clay minerals).

4.2. Mercury bound to soil organic matter (SOM)

To understand whether the peak at 240 °C was due to Hg-bound SOM, H_2O_2 was added to the soil (silicate, carbonate and peat) samples. Once the reaction between the soil samples and H_2O_2 was over, the samples were dried at a controlled temperature of 30 ± 1 °C. It is worth noting that in the oven, a tiny superficial reddish (Fe-rich) layer of oxidation in the silicate soil sample formed whilst the subsurface had a yellowish color. No layering was observed in the carbonate and peat soils, likely due to a minor amount of iron (2.36 wt%) with respect to that characterizing the silicate (Fe = 9.7 wt%) and peat soils. Therefore, the Hg speciation was carried out on both layers. The respective thermograms are reported in Fig. 6A, B, C.

By comparing the thermograms of Figs. 4A and 6A, the layer less affected by alteration always shows the main peak at about 240 °C. This suggests that the previously formed Hg^{2+} species was not related to SOM, whose concentrations was 8 wt%. The same consideration applies to the carbonate soil (Fig. 5A and 6B), which had 4 wt% of organic matter. If we compare the TD of the reddish layer (Fig. 6A) with those reported in Fig. 4A, part of the peak attributed to β-HgS is still occurring, though in a smaller quantity. Nevertheless, a new peak, shifted by about 50 °C with respect to the green line (Fig. 6A), is formed, reaching a maximum release temperature of 305 ± 5 °C. During the reaction of the silicate soil with H_2O_2, part of β-HgS is oxidized to form SO_4^{2-}, while Hg^{2+} ions are released according to the reaction (2) and probably bound to the presence of Fe–Al or Mn oxides in the soil, whilst part of the β-HgS is not affected by oxidization.

$$HgS_s + 4H_2O_2 \rightarrow Hg^{2+} + SO_4^{2-} + 4H_2O \qquad (2)$$
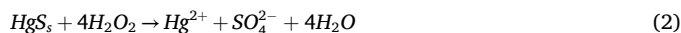
As reported by Han et al. (2017), the presence of thiophilic metals (e. g. Cu^+, Fe^{2+}) involves the displacement of Hg^{2+} from HgS to Hg $(S_2O_3)_n^{2-2n}$. Given the generally high metal (e.g. Cu^+, Fe^{2+}) availability in mining environments, this displacement of Hg^{2+}-induced HgS dissolution is potentially significant (Chen et al., 2018). Additionally, monodentate-bound thiosulfate ions ($S_2O_3^{2-}$) were discovered to be an oxidation intermediate on the HgS surface, which would help adsorbed Hg^{2+} to be released more easily (Holley et al., 2007), although dissolved Hg^{2+} can be re-adsorbed on the HgS surface afterward (Barnett et al., 2001; Jiang et al., 2016). It should also be pointed out that the more oxidized layer has a significantly higher THg concentration (53.4 mg/kg) with respect to that of the underlying and less altered sample (5.06 mg/kg).

The peat soil, characterized by a concentration of SOM of about 75 wt% (Fig. 6C), does not show the peak at 240 °C (Fig. 6B), but only that
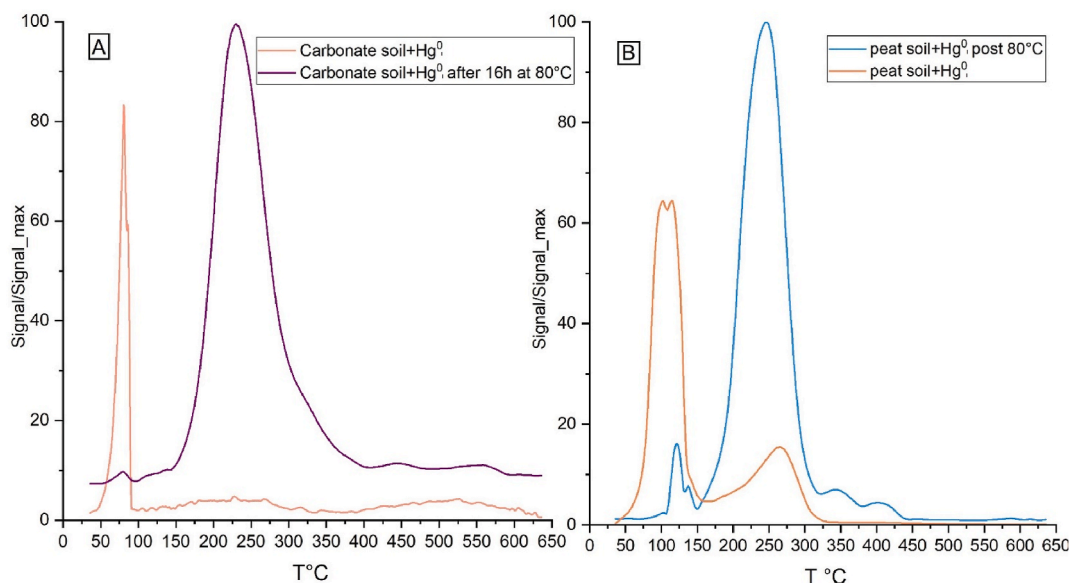

Fig. 5. A) Thermogram of carbonate soil after the addition of Hg_l^0 at time 0 and after heating at 80 °C for 16 h; B) thermogram of peat soil after the addition of Hg_l^0 at time 0 and after heating at 80 °C for 16 h.
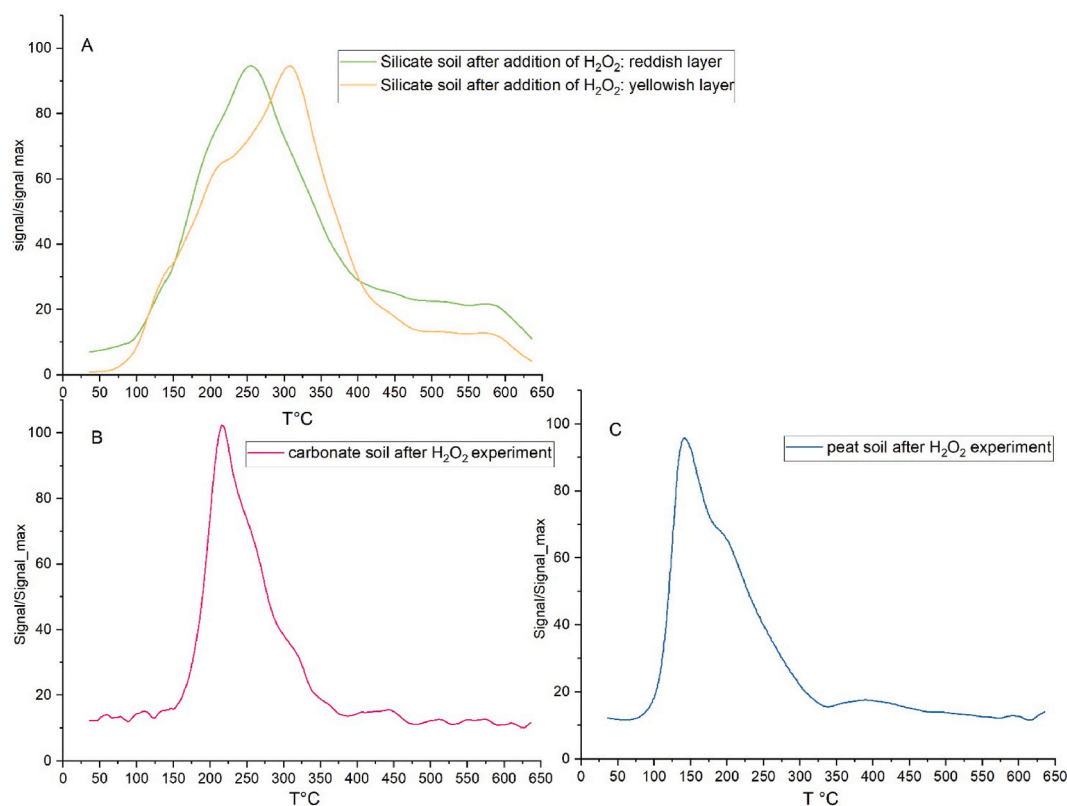
Fig. 6. A) Thermogram of silicate soil after the addition of Hg_l^0 and the removal of organic matter by H_2O_2. The two peaks refer to the alteration stratification observed in the 15 mL falcon-like vial after drying at 30 °C. The term "reddish" refers to the superficial (more altered) layer whereas the term "yellowish" indicates the lower and less altered part of the silicate soil (see text). B) Thermogram of carbonate soil after the addition of Hg_l^0 and the removal of organic matter by H_2O_2. C) Thermogram of peat soil after the addition of Hg_l^0 and the removal of organic matter by H_2O_2.

at 150 °C. According to Gonzalez-Raymat et al. (2017), SOM may form Hg^{2+}-complexes. Consequently, electrons are transferred from the organic matter to Hg^{2+} to form Hg^0. In this case, Hg^{2+} was not reduced to Hg^0, but to Hg^+. On the other hand, Hg^+ is not a stable form since, under atmospheric conditions (Galbreath and Zygarlicke, 1996), can easily be oxidized or reduced to Hg^{2+} or Hg^0, respectively. Ravichandran (2004) and Skyllberg et al. (2000) noted that soils rich in organic matter can increase the mobility of Hg through the formation of Hg organo-complexes, favoring the mobility of Hg in interstitial soil waters that ultimately may be transferred to the shallow aquifers. Differently, the carbonate soil does not present any changes after the reaction with H_2O_2, confirming that this peak is not related to organic matter.

5. Conclusions

Different experimental TD runs were carried out by coupling Lumex RA-915 M and Pyro 915+ instrumentations for defining the breakdown temperatures of different Hg-standards, which were then mixed with pure $CaCO_3$ and a Hg-free silicate soil and further analyzed along with carbonate-, silicate- and organic matter-rich soils mixed with liquid Hg. Previous studies on similar matrices are in agreement with our results, whereas, to the best of our knowledge, no attempts have previously been performed with liquid Hg mixture at room temperature to define the products derived by thermo-desorption profiles. It has been evidenced that Hg^0 suffers oxidation processes to form more stable species (e.g. Hg^{2+}) in a relatively short time (~42 days) and the desorption temperatures of the different Hg-bearing compounds result to be modified with respect to those determined by using pure Hg-compounds. Transient Hg^+ forms were also recognized before the complete oxidation of Hg^0. Further studies are claimed to focus on the processes occurring between liquid Hg and different soil matrices. Nevertheless, these results

are expected to have important implications during soil remediation activities in areas where mercury has been used for industrial purposes or exploited from presently decommissioned mining activities. According to the different Hg-species occurring in soil, cautions are to be used during inertization processes or in-situ or ex-situ treatments. The presence of Hg^0 and/or unstable products may produce unwanted reactions that may jeopardize the quality of the resulting material. Future studies may be focused on the characterization of the soil organic matter and the effects that SOM and the microbial activity are expected to suffer by the presence of liquid mercury.

CRediT authorship contribution statement

Federica Meloni: Writing – review & editing, Writing – original draft, Visualization, Validation, Methodology, Investigation, Formal analysis, Data curation, Conceptualization. **Pablo L. Higueras:** Writing – review & editing, Writing – original draft, Supervision, Resources, Methodology, Investigation, Conceptualization. **Jacopo Cabassi:** Writing – review & editing, Writing – original draft, Visualization, Validation, Methodology, Conceptualization. **Barbara Nisi:** Writing – review & editing, Writing – original draft, Visualization, Validation, Resources, Methodology, Investigation, Data curation, Conceptualization. **Daniele Rappuoli:** Writing – review & editing, Writing – original draft, Resources, Funding acquisition. **Orlando Vaselli:** Writing – review & editing, Writing – original draft, Validation, Supervision, Project administration, Methodology, Investigation, Funding acquisition, Formal analysis, Data curation, Conceptualization.

Declaration of competing interest

The authors declare that they have no known competing financial

interests or personal relationships that could have appeared to influence the work reported in this paper.

Data availability

Data will be made available on request.

Acknowledgements

Appendix A. Supplementary data

Supplementary data to this article can be found online at https://doi.org/10.1016/j.chemosphere.2024.143349.

References

AMAP/UNEP, 2013. Technical Background Report for the Global Mercury Assessment 2013. Arctic Monitoringand Assessment Programme, Oslo, Norway/UNEP Chemicals Branch, Geneva, Switzerland vi + 263.

Ariya, P.A., Amyot, M., Dastoor, A., Deeds, D., Feinberg, A., Kos, G., Poulain, A., Ryjkov, A., Semeniuk, K., Subir, M., Toyota, K., 2015. Mercury physicochemical and biogeochemical transformation in the atmosphere and at atmospheric interfaces: a review and future directions. Chem. Rev. 115, 3760–3802. https://doi.org/10.1021/cr500667e.

Azevedo, R., Rodriguez, E., 2012. Phytotoxicity of mercury in plants: a review. J. Bot., Le 848614. https://doi.org/10.1155/2012/848614.

Baldi, F., Olson, G.J., Brinckman, F.E., 1987. Mercury transformations by heterotrophic bacteria isolated from cinnabar and other metal sulfide deposits in Italy. Geomicrobiol. J. 5, 1–16.

Barnett, M.O., Turner, R.R., Singer, P.C., 2001. Oxidative dissolution of metacinnabar (beta-HgS) by dissolved oxygen. Appl. Geochem. 16, 1499–1512. https://doi.org/10.1016/S0883-2927(01)00026-9.

Biester, H., 1994. Moglichkeiten der Anwendung eines temperaturgesteuerten Pyrolyseverfahrenszur Bestimmung der Bindungsform des Quecksilbers in Boden und Sedimenten, vol. 75. Ph.D. Dissertation, Heidelberg; Germany, p. 156. S.

Biester, H., Gosar, M., Müller, G., 1999. Mercury speciation in tailings of the Idrija mercury mine. J. Geochem. Explor. 65195–65204. https://doi.org/10.1016/S0375-6742(99)00027-8.

Biester, H., Scholz, C., 1996. Determination of mercury binding forms in contaminated soils: mercury pyrolysis versus sequential extractions. Environ. Sci. Technol. 31, 233–239. https://doi.org/10.1021/es960369h.

Bouffard, A., Amyout, M.A., 2008. Importance of elemental mercury in lake sediments. Chemosphere 74, 1098–1103. https://doi.org/10.1016/j.chemosphere.2008.10.045.

Cabassi, J., Rimondi, V., Yeqing, Z., Vacca, A., Vaselli, O., Buccianti, A., Costagliola, P., 2020. 100 years of high GEM concentration in the central Italian herbarium and tropical herbarium studies centre (florence, Italy). J. Environ. Sci. 87, 377–388. https://doi.org/10.1016/j.jes.2019.07.007.

Cabassi, J., Venturi, S., Di Bennardo, F., Nisi, B., Tassi, F., Magi, F., Ricci, A., Picchi, G., Vaselli, O., 2021. Flux measurements of gaseous elemental mercury (GEM) from the geothermal area of "Le Biancane" natural park (Monterotondo Marittimo, Grosseto, Italy): biogeochemical processes controlling GEM emission. J. Geochem. Expl. 228 https://doi.org/10.1016/j.gexplo.2021.106824.

Chen, Y., Yin, Y., Shi, J., Liu, G., Hu, L., Liu, J., Cai, Y., Jiamg, G., 2018. Analytical method, formation, and dissolution of cinnabar and its impact on environmental cycle of mercury. Crit. Rev. Environ. Sci. Technol. 1–33. https://doi.org/10.1080/10643389.2018.1429764.

Coufalík, P., Zvěřina, O., Komárek, J., 2014. Determination of mercury species using thermal desorption analysis in AAS. Chem. Pap. 68, 427–434. https://doi.org/10.2478/s11696-013-0471-0.

Debure, M., Grangeon, S., Robinet, J.C., Madé, B., Fernández, A.M., Lerouge, C., 2020. Influence of soil redox state on mercury sorption and reduction capacity. Sci. Tot. Environ. 2 707, 136069 https://doi.org/10.1016/j.scitotenv.2019.136069.

Do Valle, C.M., Santana, G.P., Widöller, C.C., 2006. Mercury conversion processes in Amazon soils evaluated by thermos desorption analysis. Chemosphere 65, 1966–1976. https://doi.org/10.1016/j.chemosphere2006.07.001.

Dong, W., Liu, J., Wei, L.X., Yang, J.F., Chernick, M., Hinton, D.E., 2016. Developmental toxicity from exposure to various forms of mercury compounds in medaka fish (Oryzias latipes) embryos. PeerJ 4, e2282. https://doi.org/10.7717/peerj.2282.

Driscoll, C.T., Mason, R.P., Chan, H.M., Jacob, D.J., Pirrone, N., 2013. Mercury as a global pollutant: sources, pathways, and effects. Environ. Sci. Technol. 47, 4967–4983. https://doi.org/10.1021/es305071v.

Du, H., Gu, X., Johs, A., Yin, X.T., Wang, D., Pierce, E.M., Gu, B., 2023. Sonochemical oxidation and stabilization of liquid elemental mercury in water and soil. J. Haz. Mat. 445, 130589 https://doi.org/10.1016/j.jhazmat.2022.130589.

Friani, R., Meloni, F., Becatti, A., 2023. Determination of Hg^0 in solid matrices: a new approach with Lumex-Pyro thermal desorption. The case study in the former mine of Abbadia San Salvatore (Mt. Amiata; Southern Tuscany; Italy). Joint Congress SGI. SIMP, SoGe.I., AIV, The Geoscience paradigm resources risks and future perspectives, Book of Abstracts 293. September 19-21, 2023 Potenza (Italy).

Fritsche, J., Obrist, D., Alewell, C., 2008. Evidence of microbial control of Hg^0 emissions from uncontaminated terrestrial soils. J. Plant Nutr. Soil Sci. 171, 200–209. https://doi.org/10.1002/jpln.200625211.

Frohne, T., Rinklebe, J., Langer, U., Du Laing, G., Mothes, S., Wennrich, R., 2012. Biogeochemical factors affecting mercury methylation rate in two contaminated floodplain soils. Biogeosciences 9, 493–507. https://doi.org/10.5194/bg-9-493-2012.

Galbreath, K.C., Zygarlicke, C.J., 1996. Mercury speciation in coal combustion and gasification flue gases. Environ. Sci. Technol. 30, 2421–2426. https://doi.org/10.1021/es950935t.

Ghani, J., Nawab, J., Khan, S., Khan, M.A., Ahmad, I., Ali, H.M., Siddiqui, M.H., Funari, V., Dinelli, E., 2024. Organic amendments minimize the migration of potentially toxic elements in soil–plant system in degraded agricultural lands. Biomass Conv. Bioref. 14, 6547–6565. https://doi.org/10.1007/s13399-022-02816-3, 2024.

Ghezzi, L., Valerio, M., Petrini, R., 2023. Novel determination of elemental mercury in silicate rock by thermal desorption. Anal. Lett. 56, 1270–1278. https://doi.org/10.1080/00032719.2022.2125984.

Gonzalez-Raymat, H., Liu, G., Liriano, C., Li, Y., Yin, Y., Shi, J., Jiang, G., Cai, Y., 2017. Elemental mercury: its unique properties affect its behavior and fate in the environment. Environ. Pollut. 229, 69–86. https://doi.org/10.1016/j.envpol.2017.04.101.

Han, C., Wang, W., Xie, F., 2017. Mechanism and Kinetics of Mercuric Sulfide Leaching with Cuprous-Thiosulfate Solutions, vol. 177. Sep. Purif. Technology, pp. 223–232. https://doi.org/10.1016/j.seppur.2017.01.001.

Hocsman, A., Di Nezio, S., Charlet, L., Avena, M., 2006. On the mechanisms of dissolution of montroydite HgO(s): dependence of the dissolution rate on pH, temperature, and stirring rate. J. Colloid Interface Sci. 297, 696–704. https://doi.org/10.1016/j.jcis.2005.11.020.

Holley, E.A., McQuillan, A.J., Craw, D., Kim, J.P., Sander, S.G., 2007. Mercury mobilization by oxidative dissolution of cinnabar (alpha-HgS) and metacinnabar (beta-HgS). Chem. Geol. 240, 313–325. https://doi.org/10.1016/j.chemgeo.2007.03.001.

Hong, Y.S., Kim, Y.M., Lee, K.E., 2012. Methylmercury exposure and health effects. J. Prev. Med. Public Health 45, 353–363. https://doi.org/10.3961/jpmph.2012.45.6.353.

Huang, Y., Zhao, B., Liu, G., Liu, K., Dang, B., Lyu, H., Tang, J., 2023. Effective reducing the mobility and health risk of mercury in soil under thiol-modified biochar amendment. J. Haz. Mat. 462, 132712 https://doi.org/10.1016/j.jhazmat.2023.132712.

Jiang, P., Li, Y.B., Liu, G.L., Yang, G.D., Lagos, L., Yin, Y.G., Baohua, G., Jiang, G., Cai, Y., 2016. Evaluating the role of re-adsorption of dissolved Hg2C during cinnabar dissolution using isotope tracer technique. J. Hazard Mater. 317, 466–475. https://doi.org/10.1016/j.jhazmat.2016.05.084.

Lin, C.J., Gustin, M.S., Singhasuk, P., Eckley, C., Miller, M., 2010. Empirical models for estimating mercury flux from soils. Environ. Sci. Technol. 44, 8522–8528. https://doi.org/10.1021/es1021735.

Liu, S., Wang, X., Guo, G., Yan, Z., 2020. Status and environmental management of soil mercury pollution in China: a review. J. Environ. Manag. 277 (2021), 111442 https://doi.org/10.1016/j.envman.2020.111442.

López, F.A., López-Delgado, A., Padilla, I., Tayibi, H., Alguacil, F.J., 2010. Formation of metacinnabar by milling of liquid mercury and elemental sulfur for long term mercury storage. Sci. Tot. Environ. 408, 4341–4345. https://doi.org/10.1016/j.scitotenv.2010.07.008.

Mashyanov, N.R., Pogarev, S.E., Panova, E.G., Panichev, N., Ryzhov, V., 2017. Determination of mercury thermospecies in coal. Fuel 203, 973–980. https://doi.org/10.1016/j.fuel.2017.03.085.

Mason, R.P., Choi, A.L., Fitzgerald, W.F., Hammerschmidt, C.R., Lamborg, C.H., Soerensen, A.L., Sunderland, E.M., 2012. Mercury biogeochemical cycling in the ocean and policy implications. Environ. Res. 119, 101–117. https://doi.org/10.1016/j.envres.2012.03.013.

Meloni, F., Farieri, A., Higueras, P.L., Esbrì, M.J., Nisi, B., Cabassi, J., Rappuoli, D., Vaselli, O., 2023. Mercury distribution in plants and soils from the former mining area of Abbadia San Salvatore (Tuscany, Central Italy). Environ. Geochem. Health 45, 8523–8538. https://doi.org/10.1007/s1065-023-01739-w.

Miller, C.L., Watson, D.B., Lester, B.P., Howe, J.Y., Phillips, D.H., He, F., Liang, L., Pierce, E.M., 2015. Formation of soluble mercury oxide coatings: transformation of elemental mercury in soils. Environ. Sci. Technol. 49 (20), 12105–12111. https://doi.org/10.1021/acs.est.5b00263.

Miller, C.L., Watson, D.B., Lester, B.P., Lowe, K.A., Pierce, E.M., Liang, L., 2013. Characterization of soils from an industrial complex contaminated with elemental mercury. Environ. Res. 125, 20–29.

Molina, J.A., Oyarzun, R., Esbrí, J.M., Higueras, P., 2006. Mercury accumulation in soils and plants in the Almadén mining district, Spain: one of the most contaminated sites on Earth. Environ. Geochem. Health 28, 487–498. https://doi.org/10.1007/s10653-006-9058-9.

Nagy, K.L., Manceau, A., Gasper, J.D., Ryan, J.N., Aiken, G.R., 2011. metallothionein-like multinuclear clusters of mercury(II) and sulphur in peat. Environ. Sci. Technol. 45, 7298–7306. https://doi.org/10.1021/es201025v.

Obrist, D., 2012. Mercury distribution across 14 U.S. forests. Part II: patterns of methyl mercury concentrations and areal mass of total and methyl mercury. Environ. Sci. Technol. 46, 5921–5930.

Obrist, D., Kirk, J.L., Zhang, L., Sunderland, E.M., Jiskra, M., Selin, N.E., 2018. A review of global environmental mercury processes in response to human and natural perturbations: changes of emissions, climate, and land use. Ambio 47, 116–140. https://doi.org/10.1007/s13280-017-1004-9, 2018.

O'Connor, D., Hou, D., Ok, Y.S., Mulder, J., Duan, L., Wu, Q., Wang, S., Tack, F.M.G., Rinklebe, J., 2019. Mercury speciation; transformation; and transportation in soils; atmospheric flux; and implications for risk management: a critical review. Environ. Int. 126, 747–761. https://doi.org/10.1016/j.envint.2019.03.019.

Padalkar, P.P., Chakraborty, P., Chennuri, K., Jayachandran, S., Sitlhou, L., Nanajkar, M., Tilvi, S., Singh, K., 2019. Molecular characteristics of sedimentary organic matter in controlling mercury (Hg) and elemental mercury (Hg0) distribution in tropical estuarine sediments. Sci. Total Environ. 668, 592–601. https://doi.org/10.1016/j.scitotenv.2019.02.353.

Petranich, E., Predonzani, S., Acquavita, A., Mashyanov, N., Covelli, S., 2022. Rapid thermoscanning technique for direct analysis of mercury species in contaminated sediments: from pure compounds to real sample application. Appl. Geochem. 143, 105393 https://doi.org/10.1016/j.apgeochem.2022.105393.

Protano, G., Nannoni, F., 2018. Influence of ore processing activity on Hg, as and Sb contamination and fractionation in soils in a former mining site of Monte Amiata ore district (Italy). Chemosphere 199, 320–330. https://doi.org/10.1016/j.chemosphere.2018.02.051.

Raposo, C., Widmöller, C.C., Durao Junior, W.A., 2023. Mercury speciation in fluorescent lamps by thermal release analysis. Waste Manage. (Tucson, Ariz.) 23, 879–886. https://doi.org/10.1016/S0956-053X(03)00089-8.

Ravichandran, M., 2004. Interactions between mercury and dissolved organic matter—a review. Chemosphere 55, 319–331. https://doi.org/10.1016/j.chemosphere.2003.11.011.

Reis, A.T., Davidson, C.M., Vale, C., Pereira, E., 2016. Overview and challenges of mercury fractionation and speciation in soils. TrAC Trends in Anal. Chem. 82, 109–117.

Rumayor, M., Diaz-Somoano, M., Lopez-Anton, M.A., Martinez-Tarazona, M.R., 2013. Mercury compounds characterization by thermal desorption. Talanta 114, 318–322. https://doi.org/10.1016/j.talanta.2013.05.059.

Rumayor, M., Gallego, J.R., Rodriguez-Valdés, E., Diaz-Somoano, M., 2017. An assessment of the environmental fate of mercury species in highly polluted brownfields using thermal desorption. J. Hazard Mater. 325, 1–7. https://doi.org/10.1016/j.jhazmat.2016.11.068.

Schuster, E., 1991. The behavior of mercury in the soil with special emphasis on complexation and adsorption processes-a review of the literature. Water Air & Soil Pollut 56, 667–680.

Sholupov, S., Pogarev, S., Ryzhov, V., Mashyanov, N., Stroganov, A., 2004. Zeeman atomic absorption spectrometer RA-915 for direct determination of mercury in air and complex matrix samples. Fuel Process. Technol. 85, 473–485. https://doi.org/10.1016/j.fuproc.2003.11.003.

Skyllberg, U., Xia, K., Bloom, P.R., Nater, E.A., Bleam, W.F., 2000. Binding of mercury (II) to reduced sulfur in soil organic matter along upland-peat soil transects. J. Environ. Qual. 29 (3), 855–865. https://doi.org/10.2134/jeq2000.00472425002900030022x.

Skyllberg, U., Drott, A., 2010. Competition between disordered iron sulphide and natural organic matter associated thiols for Mercury(II)-an EXAFS study. Environ. Sci. Technol. 44, 1254–1259. https://doi.org/10.1021/es902091w.

Skyllberg, U., 2008. Competition among thiols and inorganic sulfides and polysulfides for Hg and MeHg in wetland soils and sediments under suboxic conditions: illumination of controversies and implications for MeHg net production. J. Geophys. Res. 113, G00C03 https://doi.org/10.1029/2008JG000745.

Sladek, C., Gustin, M.S., 2003. Evaluation of sequential and selective extraction methods for determination of mercury speciation and mobility in mine waste. Appl. Geochem. 18, 567–576. https://doi.org/10.1016/S0883-2927(02)00115-4.

UNEP, 2009. Global atmospheric mercury assessment: sources, emission and transport. Retrieved from: https://wedocs.unep.org/bitstream/handle/20.500.11822/11517/UNEP_GlobalAtmosphericMercuryAssessment_May2009.pdf?sequence=1&isAllowed=y.

Vaselli, O., Lazzaroni, M., Nisi, B., Cabassi, J., Tassi, F., Rappuoli, D., Meloni, F., 2021. Discontinuous geochemical monitoring of the galleria italia circumneutral waters (former Hg-mining area of Abbadia san Salvatore, tuscany, Central Italy) feeding the fosso della chiusa creek. Environments 8, 15. https://doi.org/10.3390/environments8020015.

Vaselli, O., Nisi, B., Rappuoli, D., Cabssi, J., Tassi, F., 2017. Gaseous Elemental mercury and total and leached mercury in building material from the former Hg-mining area of Abbadia San Salvatore (Central Italy). Int. J. Environ. Res. Public Health 14, 425. https://doi.org/10.3390/ijerph14040425.

Vezzoli, L., Principe, C., 2023. Building a silicic effusive volcano: geology, structure, and tectonics of monte Amiata (middle pleistocene, Italy). J. Volcanol. Geotherm. Res. 434, 107743 https://doi.org/10.1016/j.jvolgeores.2022.107743.

Wang, L., Hou, D., Cao, Y., Sik Ok, Y., Tack, F.M.G., Rinklebe, J., O'Connor, D., 2020. Remediation of mercury contaminated soil, water, and air: a review of emerging materials and innovative technologies. Environ. Int. 134, 105281 https://doi.org/10.1016/j.envint.2019.105281.

Wang, Y., Li, Y., Liu, G., Wang, D., Jiang, G., Cai, Y., 2015. Elemental mercury in natural waters: occurrence and determination of particulate Hg^0. Environ. Sci. Technol. 49 (16), 9742–9749. https://doi.org/10.1021/acs.est.5b01940.

WHO, 2017. Ten chemicals of major health concern. from. www.who.int/ipcs/assessment/public_health/chemicals_phc/en/index.html.

Widmöller, C.C., Wilken, R.D., De Figueiredo Jardim, W., 1996. Mercury speciation in contaminated soils by thermal release analysis. Water Air soil Pollut 89, 399–416, 1996.

Widmöller, C.C., Durão Junior, W., de Oliveira, A., do Valle, C.M., 2015. The redox processes in Hg-contaminated soils from Descoberto (Minas Gerais; Brazil): implications for the mercury cycle. Ecotoxicol. Environ. Saf. 112, 201–211. https://doi.org/10.1016/j.ecoenv.2014.11.009.

Widmöller, C.C., Silva, N.C., Morai Andrade, P.H., Mendes, L.A., do Valle, C.M., 2017. Use of a direct mercury analyzer for mercury speciation in different matrices without sample preparation. Anal. Methods 9, 2159. https://doi.org/10.1039/c6ay03041f.

Wu, Y.-S., Osman, A.I., Hosny, M., Elgarahy, A.M., Eltaweil, A.S., Rooney, D.W., Chen, Z., Rahim, N.S., Sekar, M., Gopinath, S.C.B., Mat Rani, N.N.I., Batumalaie, K., Yap, P.-S., 2024. ACS Omega 9, 5100–5126. https://doi.org/10.1021/acsomega.3c07047, 2024.

Wu, S., Uddin, M.A., Nagano, S., Ozaki, M., Sasaika, E., 2015. Fundamental Study on Decomposition Characteristics of Mercury Desorption Mass Spectrometry, vol. 2011. Springer, Singapore.

Xu, J., Garcia Bravo, A., Lagerkvist, S., Bertilsson, S., Sjöblom, R., Kumpiene, J., 2015. Sources and remediation techniques for mercury contaminated soil. Environ. Int. 4, 42–53. https://doi.org/10.1016/j.envint.2014.09.007.